Characterization of water-soluble brown carbon chromophores from wildfire plumes in the western US using size exclusion chromatography

Lisa Azzarello[1], Rebecca A. Washenfelder[2], Michael A. Robinson[2,3], Alessandro Franchin[2,3,4], Caroline C. Womack[2,3], Christopher D. Holmes[5] Steven S. Brown[2,6], Ann Middlebrook[2], Tim Newberger [7], Colm Sweeney [7], Cora J. Young[1]

[1]Department of Chemistry, York University, Toronto, ON, M3J 1P3, Canada

[2]Chemical Sciences Laboratory, National Oceanic and Atmospheric Administration, 325 Broadway, Boulder, CO 80305, USA

[3]Cooperative Institute for Research in Environmental Sciences (CIRES), University of Colorado, Boulder, CO, 80309, USA

[4]Now at: National Center for Atmospheric Research, Boulder, CO, USA

[5]Earth, Ocean, and Atmospheric Science, Florida State University, Tallahassee, FL 32304, USA

[6]Department of Chemistry, University of Colorado Boulder, Boulder, Colorado, USA

[7]Global Monitoring Laboratory, National Oceanic and Atmospheric Administration, 325 Broadway, Boulder, CO 80305, USA

Correspondence to: C. J. Young (youngcj@yorku.ca)

Abstract

Wildfires are an important source of carbonaceous aerosol in the atmosphere. Organic aerosol that absorbs light in the ultraviolet to visible spectral range is referred to as "brown carbon" (BrC), and its impact on Earth's radiative budget has not been well characterized. We collected water-soluble brown carbon using a particle into liquid sampler (PILS) onboard a Twin Otter aircraft during the Fire Influence on Regional to Global Environments and Air Quality (FIREX-AQ) campaign. Samples were collected downwind of wildfires in the western United States from August to September 2019. We applied size exclusion chromatography (SEC) with ultraviolet-visible spectroscopy to characterize the molecular size distribution of BrC chromophores. The wildfire plumes had transport ages of 0 to 5 h and the absorption was dominated by chromophores with molecular weights <500 Da. With BrC normalized to a conserved biomass burning tracer, carbon monoxide, a consistent decrease in BrC absorption with plume age was not observed during FIREX-AQ. These findings are consistent with the variable trends in BrC absorption with plume age reported in recent studies. While BrC absorption trends were broadly consistent between the offline SEC analysis and the online PILS measurements, the absolute values of absorption and their spectral dependence differed. We investigate plausible explanations for the discrepancies observed between the online and offline analyses. This included solvent effects, pH, and sample storage. We suspect that sample storage impacted the absorption intensity of the offline measurements without impacting the molecular weight distribution of BrC chromophores.

1. Introduction

The wildfire season across the western United States has greatly intensified over the past century. The U.S. Forest Service reports that the amount of western U.S. land burned by "high severity" wildfires (i.e., fires that destroy more than 95% of vegetation) has increased eightfold since 1985 (Parks and Abatzoglou, 2020). A variety of factors influence the number and intensity of wildfires, including fuel availability, temperature, drought conditions, location of lightning strikes, and direct human influence. During the 20th century, fire suppression tactics were applied throughout the western U.S. and these efforts caused fuel to accumulate (Marlon et al., 2012). The combination of dry conditions, warmer temperatures, and fuel availability contributes to the intensity of present-day wildfires in the western U.S. Consequently, the impact that these climatic conditions have on wildfire activity has been established. However, feedback effects that wildfires have on climate is an ongoing area of research.

Wildfires emit carbonaceous particulate matter into the atmosphere (Bond et al., 2004; van der Werf et al., 2010). Based on volatility and optical properties, carbonaceous aerosol particles emitted from biomass burning are categorized as elemental carbon (EC) and organic carbon (OC) (Turpin et al., 1990). Elemental carbon, referred to as black carbon (BC), is refractory and is characterized by broad absorbance across the ultraviolet (UV) to infrared wavelengths (Seinfeld and Pankow, 2003; Andreae and Gelencsér, 2006; Laskin et al., 2015). The light-absorbing components of organic aerosols are referred to as brown carbon (BrC) (Laskin et al., 2015). The direct absorption and scattering of solar radiation by these aerosol particles impacts the global radiative budget (Boucher, O.; Randall, D.; Artaxo, P.; Bretherton, C.; Feingold et al., 2013; Forster, P.; Ramaswamy, V.; Artaxo, P.; Berntsen, T.; Betts et al., 2007), but there is uncertainty about the magnitude of this effect. Currently, more information is known about BC and its impact on climate than BrC, as BrC is more chemically complex and more reactive (Buis, 2021; Di Lorenzo et al., 2017). The direct radiative forcing of BC has been estimated to be the second largest anthropogenic climate forcing species (Ramanathan and Carmichael, 2008) and studies have suggested that BrC can contribute between 20 to 40 % to positive radiative forcing from total carbonaceous absorbing aerosol (Feng et al., 2013; Zhang et al., 2017; Zeng et al., 2020a).

Wildfire emissions are a dominant primary source of BrC (Washenfelder et al., 2015). The brown colour results from a combination of species with varying abilities to absorb light in the UV-visible region (from highly to weakly absorbing) (Hems et al., 2021). The pyrolysis of lignin

and cellulose contributes to the major chemical constituents in wildfire plumes, such as phenolic compounds and organic acids (Simoneit, 2002; Xie et al., 2019; Smith et al., 2014). Lignin pyrolysis products with aromatic functionalities absorb visible light and may contribute to the absorption properties of BrC (Hems et al., 2021). Secondary processes also contribute to BrC formation. The generation of secondary organic aerosol (SOA) stemming from gas phase reaction products includes nitration of aromatic compounds in the presence of NO_x or NO_3 (Harrison et al., 2005; Finewax et al., 2018; Xie et al., 2017). For example, catechol can react with either the NO_3 or OH radical to form 4-nitrocatechol (Finewax et al., 2018) and oxidation of toluene under elevated NO_x conditions has been observed to form over 15 absorbing compounds with nitroaromatics contributing up to 60% of absorption in the visible region (Liu et al., 2016). Although there are hypotheses about the identity of BrC chromophores, up to 40% of BrC constituents remain unidentified (Lin et al., 2017; Bluvshtein et al., 2017).

To characterize the absorbing constituents that contribute to BrC absorption, reverse phase high performance liquid chromatography (HPLC) coupled to high resolution mass spectrometry has been applied (Fleming et al., 2020). However, fresh and aged BrC consist of extremely low volatile organic compounds (ELVOCs) that may be irreversibly retained on a traditional C_{18} reverse phase HPLC column (Di Lorenzo and Young, 2016). Size exclusion chromatography coupled to ultraviolet-visible absorption spectroscopy (SEC-UV) has been demonstrated as an alternative that successfully measures the absorption properties of high and low molecular weight (MW) ELVOCs in fresh and aged biomass burning-derived samples (Di Lorenzo and Young, 2016; Di Lorenzo et al., 2017; Wong et al., 2019). Analysis by SEC-UV has been previously applied to samples collected during ground-based field measurement campaigns, where the method has established the quantification of BrC absorbance as a function of MW and provided insight into the composition of BrC. High MW (>400 Da) compounds with unknown structural identities have been determined to contribute to BrC absorption and the relative contribution to BrC absorption by high MW species increases with smoke age (Di Lorenzo et al., 2017; Wong et al., 2017, 2019). These findings suggested that lower MW species are less persistent in biomass burning smoke relative to higher MW species, likely due to volatilization, oxidation, polymerization, or other processes (Di Lorenzo et al., 2017; Hems et al., 2021).

The Fire Influence on Regional to Global Environments and Air Quality (FIREX-AQ) field campaign examined the impact of wildfires on atmospheric chemistry and air quality in the western

United States. In this work, we present the SEC-UV analysis of water-soluble BrC that was collected on board the National Oceanic and Atmospheric Administration (NOAA) Twin Otter aircraft during plume transects downwind from western U.S forest fires. These represent the first aircraft samples analyzed by SEC-UV to characterize BrC. We compare the total absorption measured in online and offline samples and assign the BrC absorption to different MW classes. Finally, we examine how the composition of the mobile phase used in the SEC-UV analysis impacts elution time and spectral features. This provides cautionary information about interpreting absorption results in studies that apply chromatographic separation in an aqueous-organic matrix.

2. Experimental Approach

2.1 Overview of the FIREX-AQ field campaign

FIREX-AQ was a multi-platform field campaign that investigated wildfire emissions in the western United States from Jul to Sep 2019. Instrumented aircraft and mobile laboratories were used to intercept and sample smoke plumes throughout multiple western U.S. states. These included a DC-8, ER-2, and two Twin Otter aircraft. This study focuses on smoke sampled by the "Chemistry" Twin Otter aircraft, which was based in Boise, Idaho, from 29 Jul to 5 Sep 2019, and briefly in Cedar City, Utah, from 19 Aug to 23 Aug 2019. The Twin Otter payload included gas and aerosol instruments to measure smoke composition, transport, and transformation. This included CO measurements by near infrared cavity ring-down spectroscopy (G2401-m; Picarro Inc., Santa Clara, CA, USA) (Crosson, 2008; Karion et al., 2013). A complete description of the payload installed on the Twin Otter can be found in Warneke et al. (2023). The payload weight limited the duration of in-flight sampling to 2.5 – 3 h, with a typical schedule of two or three flights per day during the afternoon, evening, or night. A total of 40 flights were completed in Arizona, Idaho, Nevada, Oregon, and Utah. Airmass back trajectory analyses were used to estimate the plume age of each transect, as described in Liao et al. (2021) and Washenfelder et al. (2022). Briefly, the smoke age was calculated by summing the horizontal advection and vertical plume rise ages between the time of emission and the aircraft interception of the smoke plume. For the Twin Otter flights, many plume intercepts by the aircraft were approximately Lagrangian (Washenfelder et al., 2022).

2.2 Online measurement of water-soluble absorption and offline sample collection

The Brown Carbon-Particle into Liquid Sampler (BrC-PILS) collected online absorption data and offline aqueous samples for the SEC-UV analysis. A complete description of the BrC-PILS instrument and sampling can be found in Zeng et al. (2021) and Washenfelder et al. (2022). Briefly, the BrC-PILS sampled smoke through a shared aerosol inlet on the Twin Otter. A parallel-plate carbon filter denuder removed volatile organic compounds prior to the aerosol entering the PILS. The PILS consisted of a steam generator and droplet impactor to collect aerosols into aqueous solution. The liquid flow then entered a liquid waveguide capillary cell (LWCC) to measure absorption. The instrument precision (3σ) for absorption at 365 nm was ±0.02 Mm^{-1} for 10 s in-flight data, with an uncertainty of ±11 % (Zeng et al., 2021). The flow exiting the LWCC was split between a total organic carbon (TOC) analyzer and an automated 14-port valve. The valve directed aqueous sample flow to one of 12 polypropylene sample tubes for offline SEC-UV analysis (Figure S1). Prior to deployment, each polypropylene tube was rinsed with 18.2 MΩ·cm deionized water (DIW) (Thermo Scientific Barnstead Smart2Pure) eight to ten times. The sample flow rate was monitored by a liquid mass flow meter prior to the flow diverting between the automated valve and the TOC analyzer. The sample flow was 1.53 mL min^{-1} during inflight sampling, and the excess 0.43 mL min^{-1} was collected into an individual polypropylene tube for 12 s to 10 min. During in-flight sampling, the flight scientist actively controlled the sample collection into each polypropylene tube to target transects of the smoke plume (example shown in Figure S2). Six to twelve aqueous samples were collected for each flight, with 201 total samples from 39 science flights. Field blanks of the DIW used to operate the BrC-PILS were stored similarly in clean polypropylene sample tubes at the beginning, halfway point, and end of campaign. Once collected in the field, the samples and blanks were stored on ice for several hours prior to refrigeration until analysis.

2.3 Offline Analysis by SEC-UV

Measurement by SEC-UV provides information about size-dependent light absorption properties of BrC chromophores. The offline aerosol samples were separated using an aqueous gel-filtration column with a MW range of 250 Da to 75 kDa (Polysep GFC P-3000, Phenomenex, Torrence, CA). Size-resolved components were detected using a diode array detector from 190 to 800 nm (UltiMate 3000, Thermo Scientific, Sunnyvale, CA) coupled to an ion chromatograph

(ICS 6000; Thermo Scientific) pump with an AS autosampler (Thermo Scientific). The isocratic method was run using a mobile phase that contained a 1:1 mixture of acetonitrile and 25 mM ammonium acetate in solution at a flow rate of 1 mL min^{-1} and a sample injection volume of 100 µL. A solution of Suwannee River Humic Acid (SRHA II, International Humic Substances Society, Saint Paul, MN, USA) was run prior to the FIREX-AQ samples to ensure proper operation of the SEC-UV set-up.

The aqueous samples collected by the BrC-PILS did not require post-sampling processing and were injected onto the SEC column under mobile phase flow to the diode array detector. The uncertainty for the offline total absorption measurements considers the uncertainty of the liquid flow and PILS collection efficiency, for a total uncertainty of ±10.5 %. Discussion of the SEC-UV method development and details of the conversion of SEC-UV signal to ambient absorption in units of Mm^{-1} can be found in the SI. We calculated BrC absorption as a function of MW by applying the calibration method described by Di Lorenzo and Young (2016) (Figure S3). Sample measurements were blank subtracted. The detection limit of the total integrated absorption (equivalent to 3σ of n=6 field blanks) was 2.5±0.2 mAU×min and 0.70±0.02 mAU×min at 250 nm and 300 nm, respectively. This corresponds to a 3σ detection limit of approximately 525 Mm^{-1} at 250 nm and 150 Mm^{-1} at 300 nm.

2.4 Absorption in different mobile phases

To assess the impact of pH and mobile-phase composition on wavelength-dependent absorption, the ammonium acetate solution was adjusted to pH 5 and pH 9 with acetic acid and ammonium hydroxide, respectively, prior to combining with acetonitrile. A 15 µg/mL in DIW solution of Suwannee River Fulvic Acid (SRFA II; International Humic Substances Society, Saint Paul, MN, USA) and a FIREX-AQ aqueous sample were injected onto the diode array detector without the SEC column in line with the following mobile phases: DIW only; 25 mM ammonium acetate solution; the default mobile phase (described in Sect. 2.3); 25 mM ammonium acetate solution adjusted to pH 5; and 25 mM ammonium acetate solution adjusted to pH 9. Solutions of 4-nitrocatechol, 4-hydroxy-3-methoxy cinnamaldehyde, vanillin, and 7-hydroxycoumarin in DIW with concentrations of 3.9×10^{-8}, 3.4×10^{-8}, 3.9×10^{-8}, 3.7×10^{-8} mol/mL, respectively, were prepared and injected onto the diode array detector to observe differences in their absorption profiles. To confirm the diode array detector results, measurements of the SRFA solution were also made with UV-visible spectroscopy (8453; Agilent Technologies, Santa Clara, CA, USA) where the solution

was mixed (1:1 ratio) with the various mobile phases prior to transferring to a cuvette for absorption measurements (Figure S7).

3. Results and discussion

3.1.Trends in absorption with plume age

We present molecular size-resolved absorption for flights that met the following criteria: (1) maximum CO concentrations greater than 0.2 ppmv; (2) three or more downwind plume transects; (3) three or more aqueous samples collected; and (4) consistent wind direction. Of the 201 aqueous samples collected, 47 samples from six flights met the criteria and are summarized in Table S1. Each aqueous sample had a measurable absorption signal in the deep UV region (250 to 300 nm), while the absorption signal above 300 nm was nearly indistinguishable from the blanks, because the samples were relatively dilute. The average (±standard deviation) integrated absorption of the 47 samples that met the criteria was 10.4±4.9 mAU×min (8134±3857 Mm^{-1}) and 0.36±0.28 mAU×min (316±214 Mm^{-1}) for 250 and 300 nm, respectively.

To account for plume dilution, we follow the convention of normalizing BrC absorption to a conserved tracer, to calculate $\Delta Abs_{\lambda,BrC}/\Delta CO$ (Forrister et al., 2015; Di Lorenzo et al., 2017; Washenfelder et al., 2022; Zeng et al., 2021; Sullivan et al., 2022), where ΔCO is the average CO mixing ratio measured during each aqueous sample collection subtracted by the average CO background outside the plume. Background BrC absorption at 365 nm (a common wavelength to report BrC absorption) was less than 0.2 Mm^{-1} and no background correction was made to determine $\Delta Abs_{\lambda,BrC}$ (Washenfelder et al., 2022). The average CO and variation of CO measured for each flight are shown in Figure S9. Figure 1 shows $\Delta Abs_{300nm,BrC}/\Delta CO$ as a function of plume age for the six selected flights, with a linear fit to each flight. The fitted slopes for $\Delta Abs_{300nm,BrC}/\Delta CO$ vs plume age vary from -0.21 to 0.88 Mm^{-1} $ppbv^{-1}$ h^{-1}, and show different trends between flights. This indicates that BrC absorption increased downwind in some plumes and decreased downwind in others.

Previous studies of normalized BrC absorption with plume age have reported conflicting results. In the earliest aircraft study, Forrister et al. (2015) collected filter samples from two fires in the western U.S. and measured the BrC absorption from water and methanol extracts. They observed that BrC absorption at 365 nm decayed exponentially over a plume age range spanning 0 to 50 h (Figure S10) (Forrister et al., 2015). Di Lorenzo et al. (2017) reported total absorption of size-resolved BrC chromophores using SEC-UV from three locations that were influenced to

varying degrees by biomass burning smoke, and observed minimal $\Delta Abs_{\lambda,BrC}/\Delta CO$ change as a function of transport times from 10 to >72 h (Figure S10). In contrast to these measurements of relatively aged biomass burning aerosol, two studies from other FIREX-AQ instruments showed different trends for relatively fresh plumes. Using BrC-PILS measurements from the Twin Otter, Washenfelder et al. (2022) showed variable trends in $\Delta Abs_{365nm,BrC}/\Delta CO$ slope values ranging from -0.02 to 0.02 Mm^{-1} $ppbv^{-1}$ h^{-1} over 0 to 5 h. Using filter samples from the DC-8 aircraft, (Zeng et al., 2022) showed that BrC increased, decreased, or was unchanged as a function of plume age over 0 to 8 h. In another study of fresh plumes, aircraft based measurements during the Western Wildfire Experiment for Cloud Chemistry, Aerosol Absorption and Nitrogen (WE-CAN; Sullivan et al., 2022) investigated the evolution of water-soluble BrC at 405 nm normalized to CO and observed BrC depletion with a smoke age of <2 h, and PILS water-soluble BrC absorption that broadly remained stable for a smoke age up to 9 h (Sullivan et al., 2022).

Our results are broadly consistent with measurements from FIREX-AQ and WE-CAN that sampled fresh plumes, and differ from the studies that sampled more aged smoke. The relatively limited plume age range of the FIREX-AQ sampling makes it challenging to deduce long-term trends associated with changes in total absorption as a function of transport time. In addition, the disparity in $\Delta Abs_{\lambda,BrC}/\Delta CO$ time dependence between FIREX-AQ observations and those reported by Forrister et al. (2015) may be attributed to i) FIREX-AQ having sampled a greater number of western U.S forest fires; and ii) the younger age of the FIREX-AQ plumes. More in-flight sampling would be required to observe BrC absorption of plume ages 5 h to 50 h to determine if the results observed by Forrister et al. (2015) would also show variability with a greater number of fires, or if the BrC lifetime would converge to a similar value.

3.2 Chemical evolution of brown carbon with plume age

Chromophores <500 Da were responsible for most of the absorption at 250-300 nm measured in the aqueous samples (Figure 2, Figure S11). For the 47 samples, molecular species >500 Da contributed an average of 3.0±1.9 % to total measured absorption at 250 nm, while molecular species <500 Da contributed an average of 72±4.5 %. Absorption past the exclusion volume represents an unidentified MW, as elution past this retention time (Figure S3) indicates non-SEC analyte-column interactions were occurring. The average contribution to total measured absorption by undefined MW species was 25.1±5.7 %. Previous SEC-UV analyses have observed elution beyond the exclusion volume and non-size exclusion effects (Wong et al., 2017; Lyu et al.,

2021). Elution at later retention times has also been observed for fresh BrC separated in a mobile phase containing 50% acetonitrile (Lyu et al., 2021). This result was attributed to non-size exclusion effects, such as hydrophobic interactions of BrC with the SEC stationary phase, which may also have contributed to elution past the exclusion volume in our samples. The absorption density plots of the aqueous samples from the flights listed in Table S1 had similar size-resolved features with varying magnitude in absorption (Figure S5).

These results are the first reported SEC-UV measurements of very fresh (0-5 h) field samples of biomass burning smoke, and they confirm some of the observations from field studies that measured more aged smoke, as well as laboratory studies that generated fresh or aged smoke. Previous studies that examined biomass burning BrC using SEC-UV have similarly concluded that fresh, less aged smoke contains a large fraction of lower MW absorbing species (Di Lorenzo et al., 2017; Wong et al., 2017; Lyu et al., 2021). In the examination of field samples, Di Lorenzo et al. (2017) collected ambient biomass burning aerosols that had been aged 10 to >72 h. They observed that low MW (<500 Da) chromophores contributed more to total absorption than higher MW (>500 Da) compounds in the least aged (10 to 15 h) biomass burning-derived filter extracts (Di Lorenzo et al., 2017). These findings resemble the absorption features of our FIREX-AQ samples, which span a plume age range from 0 to 5 hours. Wong et al. (2019) used SEC-UV to analyze filter extracts collected during fire seasons in Greece with atmospheric ages of 1 to ~70 h and observed that high MW species dominated total BrC absorption of the fresh and aged smoke. Differences between the FIREX-AQ aqueous samples and the results presented by Wong et al. (2019) can be driven by varying types of fuel emissions, photochemical conditions, meteorology, and differences in back trajectory analyses.

Two studies have applied SEC-UV analysis to lab-generated or lab-aged smoke samples. Wong et al. (2017) pyrolyzed dry hardwood and aged the samples from 0 to 10 h with UV light. They found that low MW chromophores dominated total absorption compared to high MW species, which is generally consistent with our observations. Lyu et al. (2021) generated biomass burning aerosol from laboratory combustion of boreal peat and also analyzed the aerosol by SEC-UV. Under the same SEC-UV separation conditions, the FIREX-AQ water aqueous samples parallel the findings of Lyu et al. (2021), with low MW BrC chromophores dominating total absorption for unaged fresh smoke and smoke aged between 0 to 5 h in the atmosphere.

3.3 Comparison of SEC-UV and BrC-PILS absorption

Online and offline absorption sampling are complimentary. The online sampling by the BrC-PILS provides continuous data with much higher time resolution (reported at 10 s), but it is limited to two measurements: water-soluble absorption as a function of wavelength and water-soluble organic carbon concentration. In contrast, offline samples can be examined using SEC-UV, C_{18} chromatography, and other analytical techniques that are not feasible onboard an aircraft. During FIREX-AQ, the BrC-PILS measured online water-soluble absorption in the same aqueous flow that was collected for offline sampling. These are the only BrC samples whose absorption was measured online and then subsequently offline during FIREX-AQ. We observe differences between the online and offline samples. First, absorption by the offline SEC-UV at wavelengths greater than 300 nm did not exceed its detection limit. To facilitate comparison of absorption magnitudes, a power law fit was applied to the BrC-PILS absorption between 315–395 nm to extrapolate absorption to 300 nm (Figure 3). The total absorption by the SEC-UV measurements is approximately an order of magnitude greater than the BrC-PILS measurements at 300 nm (Figure 3). To determine if the differences could be attributed to differences in the diode array detector from the SEC-UV analysis and the BrC-PILS spectrometer, a standard solution of 4-nitrocatechol was run on both systems in pure water (without the SEC column in line and bypassing the PILS). At 350 nm, the agreement between the online, offline, and literature measurements of 4-nitrocatechol absorption was ±2.1% (Figure S13) (Hinrichs et al., 2016).

The comparison between the online and offline work presented here can be compared to previous non-co-located online-offline intercomparison studies. Di Lorenzo et al. (2017) compared offline absorption measurements of filter extracts by SEC-UV to PILS-LWCC online measurements during the Southern Oxidant and Aerosol Study (SOAS). Although the SEC-UV offline samples and online measurements during SOAS were not co-located, a median ratio (SEC-UV offline at 300 nm to PILS-LWCC online at 365 nm) of 0.9 and r^2 of 0.53 (Figure S12). Zeng et al. (2021) also present an online-offline absorption comparison of water-soluble BrC collected on board the NASA DC-8 aircraft during FIREX-AQ. Online absorption measurements by a LWCC and aqueous filter extracts injected onto a LWCC offline showed good agreement at 365 nm ($r^2 = 0.84$). The correlation suggested that the filter measurement of BrC is not significantly influenced by possible sampling artifacts associated with absorption of gases or evaporative loss of BrC components associated with filter collection (Zeng et al., 2021).

Differences observed in the FIREX-AQ aqueous samples indicate the necessity to investigate a potential explanation for these inconsistencies. Since the online BrC-PILS and offline SEC-UV samples represent the same samples, solubilization differences between aerosol collection methods cannot explain the variability observed between our measurements. Although reasonable agreement between online measurements and offline filter analyses has been demonstrated (Di Lorenzo et al., 2017; Zeng et al., 2021), Resch et al. (2023) indicated that filter extracts that are not refrigerated immediately or extracts that remain refrigerated for an extended storage time are susceptible to compositional changes. For logistical reasons, our aqueous samples were collected into polypropylene tubes in the field and were not immediately subjected to controlled refrigeration or to the SEC-UV analysis. The greater absorption observed by the SEC-UV analysis (Figure 3) could reflect the possible hydrolysis of oligomeric compounds stored in aqueous solution resulting in an increase the intensity of precursor monomers as decomposition products (Resch et al., 2023). We consider this, as well as other potential causes for the differences in the next section.

3.4 Investigating the impact of solvent effects, pH, and storage effects on absorption spectra

The analysis of fresh biomass burning samples by SEC-UV may be affected by mobile phase solvation effects, pH, and sample storage conditions. We analyze and discuss these variables below and make recommendations for SEC-UV analysis. Plausible chemical structures of chromophores responsible for BrC absorption have been identified and consist of conjugated systems functionalized with hydroxyls, amines, nitro, carbonyls, and carboxylic acid groups (Laskin et al., 2015; Hems et al., 2021; Lin et al., 2017; Fleming et al., 2020; Zeng et al., 2020b; Hettiyadura et al., 2021; Marrero-Ortiz et al., 2019; De Haan et al., 2018; Ji et al., 2022). The molecular complexities of BrC species may be susceptible to changes in the absorption spectra depending on the analysis conditions.

First, we assess solvation effects due to changes in the mobile phase composition. The PILS solubilizes BrC in pure water for the online measurements to facilitate absorption measurements (Weber et al., 2001). In contrast, the mobile phase used for the offline SEC-UV analysis was a mixture of acetonitrile and DIW with 25 mM ammonium acetate. Chromatographic packing materials are often incompatible with pure water and require a mixture with an organic solvent to elute compounds from the stationary phase or, in SEC separations, to prevent sorption to the stationary phase. For this reason, chromatographic partitioning-based separations occur in

aqueous-organic mixtures, where the composition can be deliberately modified to optimize interactions of the target molecules between the stationary phase and mobile phase. In SEC, non-size exclusion interactions between the analyte and stationary phase are dominated by electrostatic and hydrophobic interactions (Hong et al., 2012). If the analyte and stationary phase are identically charged, ion exclusion effects can occur, resulting in an earlier elution time as the analyte is prevented from entering the pores. If the analyte and stationary phase are oppositely charged, adsorption can result, leading to a later elution time. Hydrophobic effects can occur if the analyte interacts with hydrophobic sites of the column matrix (Hong et al., 2012). The purpose of adding ammonium acetate to the mobile phase is to increase the ionic strength of the mobile phase and facilitate ion-pairing, which suppresses electrostatic interactions between the stationary phase and the polar and charged functional groups. The organic solvent used in our mobile phase was acetonitrile, which has been shown to be unreactive towards typical BrC components and has been recommended as an inert solvent for BrC extraction and analysis (Walser et al., 2008; Bateman et al., 2008; Chen et al., 2022). Therefore, we do not expect the mobile phase to chemically alter BrC compounds while effective at mitigating column stationary phase-analyte interactions.

While chemical changes caused by our mobile phase are unlikely, it is possible that other solvent effects on absorption could be occurring. Effects of solvent on molecular absorption are well established in the photochemistry literature (Lignell et al., 2014; Mo et al., 2017; Zheng et al., 2018; Lyu et al., 2021; Chen et al., 2022; Dalton et al., 2023). The polarity of the solvent affects the absorption wavelength by changing stabilization of the ground and/or excited states. With a decrease in solvent polarity, (acetonitrile-water is less polar relative to pure water), this can lead to a decrease in stabilization of the ground state of BrC compounds (such as 4-nitrocatchol), but this effect is molecule-dependent. The impact of solvation on red and blue spectral shifting will likely be several nanometers, which could contribute to the observed differences in the offline and online absorption measurements. Previous work has shown that acetonitrile could disrupt π- π interactions between BrC molecules, which could cause the liberation of adsorbed low MW BrC chromophores from larger chromophores or disrupt BrC aggregates (Lyu et al., 2021). Smaller, less conjugated systems typically absorb in the ultraviolet-blue wavelength region, and their $\pi \rightarrow \pi^*$ transition red shifts when more conjugated systems are fused together (Gorkowski et al., 2022). Thus, we would expect absorption measurements in the presence of acetonitrile to be blue-shifted relative to those in pure water. This represents a possible explanation for greater absorption

intensity at lower wavelengths measured in the offline SEC-UV analysis compared to the online analysis.

Second, we assess the pH of the sample matrix, which is known to affect the absorption profile of BrC compounds. Multiple studies have investigated the impact of pH on wavelength-dependent absorption. For example, Phillips et al. (2017) directly adjusted the pH of SRFA and biomass-burning derived aqueous extracts (with sodium hydroxide or hydrochloric acid) and observed no measurable shift in the spectra to shorter or longer wavelengths; however they did observe that as the pH increased, there was an increase in the magnitude of absorption, which was more pronounced at higher wavelengths. The pH of the default mobile phase solution was 7.2, while the pH of the deionized water solutions in the PILS was approximately 5 (due to carbon dioxide dissolution). To investigate the impact pH has on BrC absorption, we measured several compounds that have been shown to contribute to BrC absorption (4-nitrocatechol, vanillin, 7-hydroxycoumarin, 4-hydroxy-3-methoxy cinnamaldehyde, and mixture of the four compounds) under different solvent and pH conditions: DIW, DIW with 25 mM ammonium acetate, as well as the mobile phase at pH 5, 7.2, and 9. When the matrix conditions have a pH greater than the pK_a of the compound in question, the species will deprotonate, resulting in a shift to longer wavelengths (Hinrichs et al., 2016). For compounds with a pK_a between 5 and 9 (i.e., 4-nitrocatechol, 7-hydroxycoumarin, vanillin), we observed this phenomenon (Figure S6). To assess the impact of pH and mobile phase on a complex mixture, we also measured the absorption of a SRFA aqueous solution and a FIREX-AQ aqueous sample with the abovementioned mobile phases (Figure 4 and Figure S8). In contrast to the individual BrC compounds, no major changes in the spectral shape were observed under different mobile phase conditions. To confirm these results, we measured the absorption of SRFA in each solvent using a separate spectrophotometer (Figure S7). This suggests that the pK_a of the majority of functional groups in the absorbing compounds present were less than 5 or above 9. Nitroaromatic compounds typically have pK_a values between 5 and 8; suggesting low levels of this class of compounds present in the aqueous samples. This observation is comparable to the online BrC-PILS analysis; for aqueous absorption, Washenfelder et al. (2022) observed the average absorption contribution at 365 nm of 4-nitrocatchol was less than 1.1 % and the summed contribution to absorption by 2-nitrophenol, 4-nitrophenol, 4-nitrocatechol, 4-nitroguaiacol, and 2,4-dinitrophenolate was less than 3.6 %. Since the absorption profile of SRFA and the FIREX-AQ sample appear similar in all mobile phase conditions, we have no evidence

405 that pH of the mobile phase in the SEC separation conditions impacts the wavelength dependent
406 absorption of the FIREX-AQ aqueous samples.

407 Third, we assess the potential effect of storage on the aqueous samples measured by SEC-UV.
408 A recent study by Resch et al. (2023) observed that biomass burning-derived filter extracts stored
409 at temperatures above freezing may undergo compositional changes that can increase in signal for
410 various compounds. Hydrolysis reactions include converting alkenes to alcohols and esters to
411 carboxylic acids, and the breakdown of oligomers. The hydrolysis of oligomers such as dimer
412 esters stored in an aqueous solution can result in an increase in precursor monomers as
413 decomposition products leading to an increase in signal (Zhao et al., 2018; Resch et al., 2023).
414 Further, ammonium and alkylamines have been observed in high levels in biomass burning
415 aerosols (Di Lorenzo et al., 2018); aqueous reactions between dicarbonyls (e.g., glyoxal,
416 methylglyoxal) with ammonium and amines may also contribute to an increase in absorption
417 intensity at pH 4 to 7 (Powelson et al., 2014; Yang et al., 2023). The FIREX-AQ aqueous samples
418 had a pH of 5 and were stored at 4 °C for two years prior to analysis. Assuming they contained
419 dicarbonyl compounds and reduced nitrogenous species, it is possible reactions leading to products
420 that can contribute to greater absorption during storage occurred. To further investigate the impacts
421 of storage on a complex aqueous mixture, we measured the absorption spectra of two SRFA
422 solutions: one freshly made and one stored for one year at 4 °C. We observed an increase in
423 absorption in the aged SRFA solution, in which integrated absorption was 39 % higher than the
424 freshly-made solution. This same effect was also observed with SRHA solutions (Figure S14).
425 Thus, it is possible that processes during storage could have led to increased absorption measured
426 in the offline SEC samples.

427 Among the three processes discussed here, we conclude that the storage of aqueous extracts is
428 the most plausible explanation for the higher absorption observed in the offline samples from
429 FIREX-AQ. If hydrolysis reactions are occurring, we might expect this to impact the MW profile
430 (i.e., SEC elution times). We examined the MW profile of freshly-made and one year-aged SRFA
431 solutions (Figure 4C). The increase in absorption with storage does not measurably affect the
432 molecular size-resolved absorption of the mixtures. The same effect was observed for SRHA
433 (Figure S14). This demonstrates that any storage-induced changes in these complex mixtures of
434 organic molecules have a minimal impact on the molecular weight relative to the wide MW range
435 of the SEC column. The MW of the BrC species would have to change by ~ 100 Da to be noticeable

on the MW scale of our separation (250 Da to 75 kDa). Such a drastic change in MW is unlikely the case in most hydrolysis reactions. Thus, our results above in which we broadly categorize MW species to be less than or greater than 500 Da are likely robust. The SEC separation of the aqueous samples signify that low MW (<500 Da) chromophores contribute more to total absorption than higher MW (>500 Da), this finding is supported by previous SEC-UV analyses of BrC aged less than 10 hrs (Di Lorenzo et al., 2017; Lyu et al., 2021). The consistent MW profiles between the freshly-made and stored solutions of SRFA and SRHA reasonably suggest that storage did not have a major impact on the MW of BrC.

4. Conclusions and implications

During FIREX-AQ, instruments onboard the NOAA Twin Otter aircraft sampled smoke plumes from wildfires in the western United States with plume ages of 0 to 5 h. The BrC-PILS measured water-soluble BrC absorption online and collected aerosol in aqueous solution for offline SEC-UV analysis. The aqueous samples were collected during downwind plume transects and the online data was collected continuously during inflight sampling. SEC-UV analysis shows that BrC absorption was dominated by chromophores <500 Da. This finding is consistent with reports of laboratory-generated fresh smoke samples. Integrated absorption at 300 nm from the SEC-UV analysis was used to calculate trends in normalized BrC absorption as a function of plume age. These trends were variable and did not show an exponential decay, which is consistent with recently published results from the FIREX-AQ field campaign that examined normalized BrC absorption trends for plumes over 0 to 10 h. Comparison of the online and offline analyses of the same aqueous extracts reveals discrepancies, specifically higher absorption intensity and absorption at lower wavelengths. These discrepancies between online and offline samples demonstrate the importance of considering the conditions in which the absorption measurements are made. The inconsistencies between the offline SEC-UV analysis and the online measurements are not explained by pH or solvent effects, but may be due to reactions occurring during storage. Although increases in absorption may occur during storage of aqueous solutions, it is less likely to impact the MW of the FIREX-AQ BrC species. This highlights that BrC species are more stable collected on filters rather than in aqueous solution and the importance of inter-comparison absorption measurements by multiple methods.

Acknowledgements

We thank Carsten Warneke, Joshua Schwarz, James Crawford, and Jack Dibb for organizing the FIREX-AQ field campaign. We thank the NOAA Aircraft Operations Center for support during the field mission. L.A. was supported by a Mitacs Globalink Research Internship and an NSERC Discovery Grant. The FIREX-AQ project was supported by the NOAA Atmospheric Chemistry, Carbon, and Climate Program (AC4). We thank Robert Di Lorenzo and Trevor VandenBoer for helpful discussions. We thank three anonymous reviewers for their insightful feedback.

Data Availability Statement

The data used in the study are publicly available at https://www-air.larc.nasa.gov/missions/firex-aq/

Competing Interests

At least one of the (co-)authors is a member of the editorial board of Atmospheric Chemistry and Physics.

References

Andreae, M. O. and Gelencsér, A.: Black carbon or brown carbon? The nature of light-absorbing carbonaceous aerosols, Atmospheric Chemistry & Physics, 6, 3131–3148, https://doi.org/10.5194/acp-6-3131-2006, 2006.

Bateman, A. P., Walser, M. L., Desyaterik, Y., Laskin, J., Laskin, A., and Nizkorodov, S. A.: The effect of solvent on the analysis of secondary organic aerosol using electrospray ionization mass spectrometry., Environ Sci Technol, 42, 7341–7346, https://doi.org/10.1021/es801226w, 2008.

Bluvshtein, N., Lin, P., Flores, M., Segev, L., Mazar, Y., Tas, E., Snider, G., Weagle, C., Brown, S., Laskin, A., and Rudich, Y.: Broadband optical properties of biomass burning aerosol and identification of brown carbon chromophores, Journal of Geophysical Research: Atmospheres, 122, 5441–5456, https://doi.org/10.1002/2016JD026230, 2017.

Bond, T. C., Streets, D. G., Yarber, K. F., Nelson, S. M., Woo, J.-H., and Klimont, Z.: A technology-based global inventory of black and organic carbon emissions from combustion, Journal of Geophysical Research: Atmospheres, 109, https://doi.org/10.1029/2003JD003697, 2004.

Boucher, O.; Randall, D.; Artaxo, P.; Bretherton, C.; Feingold, G. ;, Forster, P.; Kerminen, V. M.; Kondo, Y.; Liao, H.; Lohmann, U. ;, and Rasch, P.; Satheesh, S. K.; Sherwood, S.; Stevens, B.; Zhang, X. Y.: Clouds and Aerosols. In: Climate Change 2013: The Physical Science Basis. Contribution of Working Group I to the Fifth Assessment Report of the Intergovernmental Panel on Climate Change, in: Climate Change 2013: The Physical Science Basis. Contribution of Working Group I to the Fifth Assessment Report of the Intergovernmental Panel on Climate Change, Cambridge University Press:, New York, NY, 2013.

Chen, K., Raeofy, N., Lum, M., Mayorga, R., Woods, M., Bahreini, R., Zhang, H., and Lin, Y.-H.: Solvent effects on chemical composition and optical properties of extracted secondary brown carbon constituents, Aerosol Science and Technology, 56, 917–930, https://doi.org/10.1080/02786826.2022.2100734, 2022.

Crosson, E. R.: A cavity ring-down analyzer for measuring atmospheric levels of methane, carbon dioxide, and water vapor, Applied Physics B, 92, 403–408, https://doi.org/10.1007/s00340-008-3135-y, 2008.

Dalton, A. B., Le, S. M., Karimova, N. V., Gerber, R. B., and Nizkorodov, S. A.: Influence of solvent on the electronic structure and the photochemistry of nitrophenols, Environ. Sci.: Atmos., 3, 257–267, https://doi.org/10.1039/D2EA00144F, 2023.

De Haan, D. O., Tapavicza, E., Riva, M., Cui, T., Surratt, J. D., Smith, A. C., Jordan, M.-C., Nilakantan, S., Almodovar, M., Stewart, T. N., de Loera, A., De Haan, A. C., Cazaunau, M., Gratien, A., Pangui, E., and Doussin, J.-F.: Nitrogen-containing, light-absorbing oligomers produced in aerosol particles exposed to methylglyoxal, photolysis, and cloud cycling, Environ. Sci. Technol., 52, 4061–4071, https://doi.org/10.1021/acs.est.7b06105, 2018.

Di Lorenzo, R. A. and Young, C. J.: Size separation method for absorption characterization in brown carbon: Application to an aged biomass burning sample, Geophysical Research Letters, 43, 458–465, https://doi.org/10.1002/2015GL066954, 2016.

Di Lorenzo, R. A., Washenfelder, R. A., Attwood, A. R., Guo, H., Xu, L., Ng, N. L., Weber, R. J., Baumann, K., Edgerton, E., and Young, C. J.: Molecular-size-separated brown carbon absorption for biomass-burning aerosol at multiple field sites, Environmental Science and Technology, 51, 3128–3137, https://doi.org/10.1021/acs.est.6b06160, 2017.

Di Lorenzo, R. A., Place, B. K., VandenBoer, T. C., and Young, C. J.: Composition of Size-Resolved Aged Boreal Fire Aerosols: Brown Carbon, Biomass Burning Tracers, and Reduced Nitrogen, ACS Earth and Space Chemistry, 2, 278–285, https://doi.org/10.1021/acsearthspacechem.7b00137, 2018.

Feng, Y., Ramanathan, V., and Kotamarthi, V. R.: Brown carbon: a significant atmospheric absorber of solar radiation?, Atmospheric Chemistry and Physics, 13, 8607–8621, https://doi.org/10.5194/acp-13-8607-2013, 2013.

Finewax, Z., de Gouw, J. A., and Ziemann, P. J.: Identification and quantification of 4-nitrocatechol formed from OH and NO_3 radical-initiated reactions of catechol in air in the presence of NOx: implications for secondary organic aerosol formation from biomass burning, Environ. Sci. Technol., 52, 1981–1989, https://doi.org/10.1021/acs.est.7b05864, 2018.

Fleming, L. T., Lin, P., Roberts, J. M., Selimovic, V., Yokelson, R., Laskin, J., Laskin, A., and Nizkorodov, S. A.: Molecular composition and photochemical lifetimes of brown carbon chromophores in biomass burning organic aerosol, Atmospheric Chemistry and Physics, 20, 1105–1129, https://doi.org/10.5194/acp-20-1105-2020, 2020.

Forrister, H., Liu, J., Scheuer, E., Dibb, J., Ziemba, L., Thornhill, K. L., Anderson, B., Diskin, G., Perring, A. E., Schwarz, J. P., Campuzano-Jost, P., Day, D. A., Palm, B. B., Jimenez, J. L., Nenes, A., and Weber, R. J.: Evolution of brown carbon in wildfire plumes, Geophysical Research Letters, 42, 4623–4630, https://doi.org/10.1002/2015GL063897, 2015.

Forster, P.; Ramaswamy, V.; Artaxo, P.; Berntsen, T.; Betts, R. ;, Fahey, D. W.; Haywood, J.; Lean, J.; Lowe, D. C.; Myhre, G. ; N., and J.; Prinn, R.; Raga, G.; Schulz, M.; Van Dorland, R.: In Climate Change 2007: The Physical Science Basis. Contribution of Working Group I to the Fourth Assessment Report of the Intergovernmental Panel on Climate Change, Cambridge University Press: Cambridge, United Kingdom and New York, NY, 2007; pp 129−243, 2007.

Gorkowski, K., Benedict, K. B., Carrico, C. M., and Dubey, M. K.: Complexities in Modeling Organic Aerosol Light Absorption., J Phys Chem A, 126, 4827–4833, https://doi.org/10.1021/acs.jpca.2c02236, 2022.

Harrison, M. A. J., Barra, S., Borghesi, D., Vione, D., Arsene, C., and Iulian Olariu, R.: Nitrated phenols in the atmosphere: a review, Atmospheric Environment, 39, 231–248, https://doi.org/10.1016/j.atmosenv.2004.09.044, 2005.

Hems, R. F., Schnitzler, E. G., Liu-Kang, C., Cappa, C. D., and Abbatt, J. P. D.: Aging of atmospheric brown carbon aerosol, ACS Earth and Space Chemistry, 5, 722–748, https://doi.org/10.1021/acsearthspacechem.0c00346, 2021.

Hettiyadura, A. P. S., Garcia, V., Li, C., West, C. P., Tomlin, J., He, Q., Rudich, Y., and Laskin, A.: Chemical composition and molecular-specific optical properties of atmospheric brown carbon associated with biomass burning., Environ Sci Technol, 55, 2511–2521, https://doi.org/10.1021/acs.est.0c05883, 2021.

Hinrichs, R. Z., Buczek, P., and Trivedi, J. J.: Solar absorption by aerosol-bound nitrophenols compared to aqueous and gaseous nitrophenols., Environ Sci Technol, 50, 5661–5667, https://doi.org/10.1021/acs.est.6b00302, 2016.

564 Hong, P., Koza, S., and Bouvier, E. S. P.: a review size-exclusion chromatography for the
565 analysis of protein biotherapeutics and their aggregates, Journal of Liquid Chromatography &
566 Related Technologies, 35, 2923–2950, https://doi.org/10.1080/10826076.2012.743724, 2012.

567 Ji, Y., Shi, Q., Ma, X., Gao, L., Wang, J., Li, Y., Gao, Y., Li, G., Zhang, R., and An, T.:
568 Elucidating the critical oligomeric steps in secondary organic aerosol and brown carbon
569 formation, Atmospheric Chemistry and Physics, 22, 7259–7271, https://doi.org/10.5194/acp-22-
570 7259-2022, 2022.

571 Karion, A., Sweeney, C., Wolter, S., Newberger, T., Chen, H., Andrews, A., Kofler, J., Neff, D.,
572 and Tans, P.: Long-term greenhouse gas measurements from aircraft, Atmospheric Measurement
573 Techniques, 6, 511–526, https://doi.org/10.5194/amt-6-511-2013, 2013.

574 Laskin, A., Laskin, J., and Nizkorodov, S. A.: Chemistry of Atmospheric Brown Carbon,
575 Chemical Reviews, 115, 4335–4382, https://doi.org/10.1021/cr5006167, 2015.

576 Liao, J., Wolfe, G. M., Hannun, R. A., St. Clair, J. M., Hanisco, T. F., Gilman, J. B., Lamplugh,
577 A., Selimovic, V., Diskin, G. S., Nowak, J. B., Halliday, H. S., DiGangi, J. P., Hall, S. R.,
578 Ullmann, K., Holmes, C. D., Fite, C. H., Agastra, A., Ryerson, T. B., Peischl, J., Bourgeois, I.,
579 Warneke, C., Coggon, M. M., Gkatzelis, G. I., Sekimoto, K., Fried, A., Richter, D., Weibring, P.,
580 Apel, E. C., Hornbrook, R. S., Brown, S. S., Womack, C. C., Robinson, M. A., Washenfelder, R.
581 A., Veres, P. R., and Neuman, J. A.: Formaldehyde evolution in US wildfire plumes during the
582 Fire Influence on Regional to Global Environments and Air Quality experiment (FIREX-AQ),
583 Atmospheric Chemistry and Physics, 21, 18319–18331, https://doi.org/10.5194/acp-21-18319-
584 2021, 2021.

585 Lignell, H., Hinks, M. L., and Nizkorodov, S. A.: Exploring matrix effects on photochemistry of
586 organic aerosols, Proceedings of the National Academy of Sciences, 111, 13780–13785,
587 https://doi.org/10.1073/pnas.1322106111, 2014.

588 Lin, P., Bluvshtein, N., Rudich, Y., Nizkorodov, S. A., Laskin, J., and Laskin, A.: Molecular
589 chemistry of atmospheric brown carbon inferred from a nationwide biomass burning event,
590 Environmental Science & Technology, 51, 11561–11570,
591 https://doi.org/10.1021/acs.est.7b02276, 2017.

592 Liu, J., Lin, P., Laskin, A., Laskin, J., Kathmann, S. M., Wise, M., Caylor, R., Imholt, F.,
593 Selimovic, V., and Shilling, J. E.: Optical properties and aging of light-absorbing secondary
594 organic aerosol, Atmospheric Chemistry and Physics, 16, 12815–12827,
595 https://doi.org/10.5194/acp-16-12815-2016, 2016.

596 Lyu, M., Thompson, D. K., Zhang, N., Cuss, C. W., Young, C. J., and Styler, S. A.: Unraveling
597 the complexity of atmospheric brown carbon produced by smoldering boreal peat using size-
598 exclusion chromatography with selective mobile phases, Environ. Sci.: Atmos., 1, 241–252,
599 https://doi.org/10.1039/D1EA00011J, 2021.

600 Marlon, J. R., Bartlein, P. J., Gavin, D. G., Long, C. J., Anderson, R. S., Briles, C. E., Brown, K.
601 J., Colombaroli, D., Hallett, D. J., Power, M. J., Scharf, E. A., and Walsh, M. K.: Long-term
602 perspective on wildfires in the western USA, Proceedings of the National Academy of Sciences,
603 109, E535 LP-E543, https://doi.org/10.1073/pnas.1112839109, 2012.

604 Marrero-Ortiz, W., Hu, M., Du, Z., Ji, Y., Wang, Y., Guo, S., Lin, Y., Gomez-Hermandez, M.,
605 Peng, J., Li, Y., Secrest, J., Zamora, M. L., Wang, Y., An, T., and Zhang, R.: Formation and
606 optical properties of brown carbon from small α-dicarbonyls and amines, Environ. Sci. Technol.,
607 53, 117–126, https://doi.org/10.1021/acs.est.8b03995, 2019.

608 Mo, Y., Li, J., Liu, J., Zhong, G., Cheng, Z., Tian, C., Chen, Y., and Zhang, G.: The influence of
609 solvent and pH on determination of the light absorption properties of water-soluble brown
610 carbon, Atmospheric Environment, 161, 90–98, https://doi.org/10.1016/j.atmosenv.2017.04.037,
611 2017.

612 Parks, S. A. and Abatzoglou, J. T.: Warmer and Drier Fire Seasons Contribute to Increases in
613 Area Burned at High Severity in Western US Forests From 1985 to 2017, Geophysical Research
614 Letters, 47, e2020GL089858, https://doi.org/10.1029/2020GL089858, 2020.

615 Phillips, S. M., Bellcross, A. D., and Smith, G. D.: Light Absorption by Brown Carbon in the
616 Southeastern United States is pH-dependent, Environ. Sci. Technol., 51, 6782–6790,
617 https://doi.org/10.1021/acs.est.7b01116, 2017.

618 Powelson, M. H., Espelien, B. M., Hawkins, L. N., Galloway, M. M., and De Haan, D. O.:
619 Brown Carbon Formation by Aqueous-Phase Carbonyl Compound Reactions with Amines and

Ammonium Sulfate, Environ. Sci. Technol., 48, 985–993, https://doi.org/10.1021/es4038325, 2014.

Ramanathan, V. and Carmichael, G.: Global and regional climate changes due to black carbon, Nat Geosci, 1, https://doi.org/10.1038/ngeo156, 2008.

Resch, J., Wolfer, K., Barth, A., and Kalberer, M.: Effects of storage conditions on the molecular-level composition of organic aerosol particles, Atmospheric Chemistry and Physics, 23, 9161–9171, https://doi.org/10.5194/acp-23-9161-2023, 2023.

Seinfeld, J. H. and Pankow, J. F.: Organic Atmospheric Particulate Material, Annual Review of Physical Chemistry, 54, 121–140, https://doi.org/10.1146/annurev.physchem.54.011002.103756, 2003.

Simoneit, B. R. T.: Biomass burning — a review of organic tracers for smoke from incomplete combustion, Applied Geochemistry, 17, 129–162, https://doi.org/10.1016/S0883-2927(01)00061-0, 2002.

Smith, J. D., Sio, V., Yu, L., Zhang, Q., and Anastasio, C.: Secondary organic aerosol production from aqueous reactions of atmospheric phenols with an organic triplet excited state, Environmental Science & Technology, 48, 1049–1057, https://doi.org/10.1021/es4045715, 2014.

Sullivan, A. P., Pokhrel, R. P., Shen, Y., Murphy, S. M., Toohey, D. W., Campos, T., Lindaas, J., Fischer, E. V., and Collett Jr., J. L.: Examination of brown carbon absorption from wildfires in the western US during the WE-CAN study, Atmospheric Chemistry and Physics, 22, 13389–13406, https://doi.org/10.5194/acp-22-13389-2022, 2022.

Turpin, B. J., Cary, R. A., and Huntzicker, J. J.: An in situ, time-resolved analyzer for aerosol organic and elemental carbon, Aerosol Science and Technology, 12, 161–171, https://doi.org/10.1080/02786829008959336, 1990.

Walser, M. L., Desyaterik, Y., Laskin, J., Laskin, A., and Nizkorodov, S. A.: High-resolution mass spectrometric analysis of secondary organic aerosol produced by ozonation of limonene, Phys. Chem. Chem. Phys., 10, 1009–1022, https://doi.org/10.1039/B712620D, 2008.

Warneke, C., Schwarz, J. P., Dibb, J., Kalashnikova, O., Frost, G., Al-Saad, J., Brown, S. S., Brewer, Wm. A., Soja, A., Seidel, F. C., Washenfelder, R. A., Wiggins, E. B., Moore, R. H., Anderson, B. E., Jordan, C., Yacovitch, T. I., Herndon, S. C., Liu, S., Kuwayama, T., Jaffe, D.,

649 Johnston, N., Selimovic, V., Yokelson, R., Giles, D. M., Holben, B. N., Goloub, P., Popovici, I.,
650 Trainer, M., Kumar, A., Pierce, R. B., Fahey, D., Roberts, J., Gargulinski, E. M., Peterson, D. A.,
651 Ye, X., Thapa, L. H., Saide, P. E., Fite, C. H., Holmes, C. D., Wang, S., Coggon, M. M., Decker,
652 Z. C. J., Stockwell, C. E., Xu, L., Gkatzelis, G., Aikin, K., Lefer, B., Kaspari, J., Griffin, D.,
653 Zeng, L., Weber, R., Hastings, M., Chai, J., Wolfe, G. M., Hanisco, T. F., Liao, J., Campuzano
654 Jost, P., Guo, H., Jimenez, J. L., Crawford, J., and The FIREX-AQ Science Team: Fire Influence
655 on Regional to Global Environments and Air Quality (FIREX-AQ), Journal of Geophysical
656 Research: Atmospheres, 128, e2022JD037758, https://doi.org/10.1029/2022JD037758, 2023.

657 Washenfelder, R., Attwood, A., Brock, C., Guo, H., Xu, L., Weber, R., Ng, N., Allen, H., Ayres,
658 B., Baumann, K., Cohen, R., Draper, D., Duffey, K., Edgerton, E., Fry, J., Hu, W., Jimenez, J.,
659 Palm, B., Romer, P., and Brown, S.: Biomass burning dominates brown carbon absorption in the
660 rural southeastern United States, Geophysical Research Letters, 42, 653–664,
661 https://doi.org/10.1002/2014GL062444, 2015.

662 Washenfelder, R. A., Azzarello, L., Ball, K., Brown, S. S., Decker, Z. C. J., Franchin, A.,
663 Fredrickson, C. D., Hayden, K., Holmes, C. D., Middlebrook, A. M., Palm, B. B., Pierce, R. B.,
664 Price, D. J., Roberts, J. M., Robinson, M. A., Thornton, J. A., Womack, C. C., and Young, C. J.:
665 Complexity in the evolution, composition, and spectroscopy of brown carbon in aircraft
666 measurements of wildfire plumes, Geophysical Research Letters, 49, e2022GL098951,
667 https://doi.org/10.1029/2022GL098951, 2022.

668 Weber, R. J., Orsini, D., Daun, Y., Lee, Y.-N., Klotz, P. J., and Brechtel, F.: A particle-into-
669 liquid collector for rapid measurement of aerosol bulk chemical composition, Aerosol Science
670 and Technology, 35, 718–727, https://doi.org/10.1080/02786820152546761, 2001.

671 van der Werf, G. R., Randerson, J. T., Giglio, L., Collatz, G. J., Mu, M., Kasibhatla, P. S.,
672 Morton, D. C., DeFries, R. S., Jin, Y., and van Leeuwen, T. T.: Global fire emissions and the
673 contribution of deforestation, savanna, forest, agricultural, and peat fires (1997–2009),
674 Atmospheric Chemistry and Physics, 10, 11707–11735, https://doi.org/10.5194/acp-10-11707-
675 2010, 2010.

676 Wong, J. P. S., Nenes, A., and Weber, R. J.: Changes in light absorptivity of molecular weight
677 separated brown carbon due to photolytic aging, Environmental Science & Technology, 51,
678 8414–8421, https://doi.org/10.1021/acs.est.7b01739, 2017.

Wong, J. P. S., Tsagkaraki, M., Tsiodra, I., Mihalopoulos, N., Violaki, K., Kanakidou, M., Sciare, J., Nenes, A., and Weber, R. J.: Atmospheric evolution of molecular-weight-separated brown carbon from biomass burning, Atmospheric Chemistry and Physics, 19, 7319–7334, https://doi.org/10.5194/acp-19-7319-2019, 2019.

Xie, M., Chen, X., Hays, M. D., Lewandowski, M., Offenberg, J., Kleindienst, T. E., and Holder, A. L.: Light Absorption of secondary organic aerosol: composition and contribution of nitroaromatic compounds., Environ Sci Technol, 51, 11607–11616, https://doi.org/10.1021/acs.est.7b03263, 2017.

Xie, M., Chen, X., Hays, M. D., and Holder, A. L.: Composition and light absorption of N-containing aromatic compounds in organic aerosols from laboratory biomass burning, Atmospheric chemistry and physics, 19, 2899–2915, https://doi.org/10.5194/acp-19-2899-2019, 2019.

Yang, L., Huang, R.-J., Shen, J., Wang, T., Gong, Y., Yuan, W., Liu, Y., Huang, H., You, Q., Huang, D. D., and Huang, C.: New Insights into the Brown Carbon Chromophores and Formation Pathways for Aqueous Reactions of α-Dicarbonyls with Amines and Ammonium, Environ. Sci. Technol., 57, 12351–12361, https://doi.org/10.1021/acs.est.3c04133, 2023.

Zeng, L., Zhang, A., Wang, Y., Wagner, N. L., Katich, J. M., Schwarz, J. P., Schill, G. P., Brock, C., Froyd, K. D., Murphy, D. M., Williamson, C. J., Kupc, A., Scheuer, E., Dibb, J., and Weber, R. J.: Global Measurements of Brown Carbon and Estimated Direct Radiative Effects., Geophys Res Lett, 47, e2020GL088747, https://doi.org/10.1029/2020GL088747, 2020a.

Zeng, L., Sullivan, A. P., Washenfelder, R. A., Dibb, J., Scheuer, E., Campos, T. L., Katich, J. M., Levin, E., Robinson, M. A., and Weber, R. J.: Assessment of online water-soluble brown carbon measuring systems for aircraft sampling, Atmospheric Measurement Techniques, 14, 6357–6378, https://doi.org/10.5194/amt-14-6357-2021, 2021.

Zeng, L., Dibb, J., Scheuer, E., Katich, J. M., Schwarz, J. P., Bourgeois, I., Peischl, J., Ryerson, T., Warneke, C., Perring, A. E., Diskin, G. S., DiGangi, J. P., Nowak, J. B., Moore, R. H., Wiggins, E. B., Pagonis, D., Guo, H., Campuzano-Jost, P., Jimenez, J. L., Xu, L., and Weber, R. J.: Characteristics and evolution of brown carbon in western United States wildfires,

Atmospheric Chemistry and Physics, 22, 8009–8036, https://doi.org/10.5194/acp-22-8009-2022, 2022.

Zeng, Y., Shen, Z., Takahama, S., Zhang, L., Zhang, T., Lei, Y., Zhang, Q., Xu, H., Ning, Y., Huang, Y., Cao, J., and Rudolf, H.: Molecular absorption and evolution mechanisms of PM2.5 brown carbon revealed by electrospray ionization fourier transform–ion cyclotron resonance mass spectrometry during a severe winter pollution episode in Xi'an, China, Geophysical Research Letters, 47, e2020GL087977, https://doi.org/10.1029/2020GL087977, 2020b.

Zhang, Y., Forrister, H., Liu, J., Dibb, J., Anderson, B., Schwarz, J. P., Perring, A. E., Jimenez, J. L., Campuzano-Jost, P., Wang, Y., Nenes, A., and Weber, R. J.: Top-of-atmosphere radiative forcing affected by brown carbon in the upper troposphere, Nature Geoscience, 10, 486–489, https://doi.org/10.1038/ngeo2960, 2017.

Zhao, R., Kenseth, C. M., Huang, Y., Dalleska, N. F., Kuang, X. M., Chen, J., Paulson, S. E., and Seinfeld, J. H.: Rapid Aqueous-Phase Hydrolysis of Ester Hydroperoxides Arising from Criegee Intermediates and Organic Acids., J Phys Chem A, 122, 5190–5201, https://doi.org/10.1021/acs.jpca.8b02195, 2018.

Zheng, D., Yuan, X.-A., Ma, H., Li, X., Wang, X., Liu, Z., and Ma, J.: Unexpected solvent effects on the UV/Vis absorption spectra of o-cresol in toluene and benzene: in contrast with non-aromatic solvents, Royal Society Open Science, 5, 171928, https://doi.org/10.1098/rsos.171928, 2018.

Figure 1. Ratio of absorption measured by SEC-UV at 300 nm to CO enhancement as a function of plume age for aqueous samples collected for six flights during FIREX-AQ 2019.

Figure 2. Absorption contribution at 300 nm of high (>500 Da), low (<500 Da), and unidentified molecular weight species for aqueous samples collected during the second flight leg on 21 Aug 2019.

Figure 3. Total absorption measured offline by the SEC-UV (at 300 nm) compared to the total absorption measured online by the BrC-PILS (extrapolated to 300 nm using a power-law fit). Each colour represents a different flight leg and each marker represents the integrated absorption at 300 nm for each aqueous sample measured by SEC-UV. The online BrC-PILS absorption measurement was averaged over the collection time of each aqueous sample. The error bars represent the total uncertainty in the online and offline measurements.

Figure 4. Absorption as a function of wavelength of (a) SRFA and (b) a FIREX-AQ aqueous sample collected on 28 Aug 2019 L3 with varying mobile phases. (c) Molecular weight profile of a freshly-made 15 μg/mL SRFA solution and the same solution one year later. The shaded region represents the coefficient of variation for absorption at each wavelength using n = 3 DIW.

Figure 1.

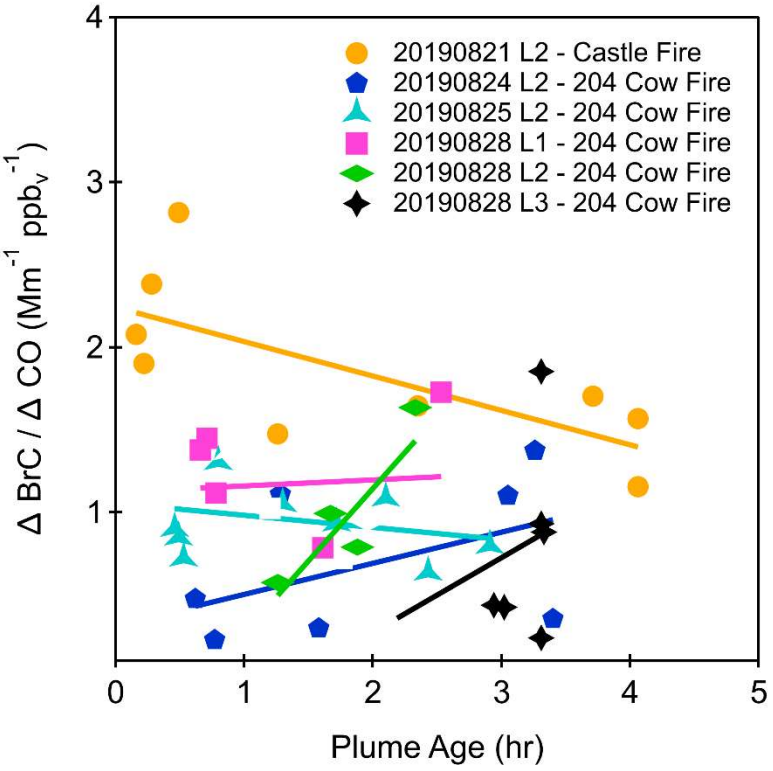
20190821 L2 - Castle Fire
20190824 L2 - 204 Cow Fire
20190825 L2 - 204 Cow Fire
20190828 L1 - 204 Cow Fire
20190828 L2 - 204 Cow Fire
20190828 L3 - 204 Cow Fire
Δ BrC / Δ CO (Mm-1 ppbv-1)
Plume Age (hr)
0
1
2
3
4
5

741 **Figure 2.**

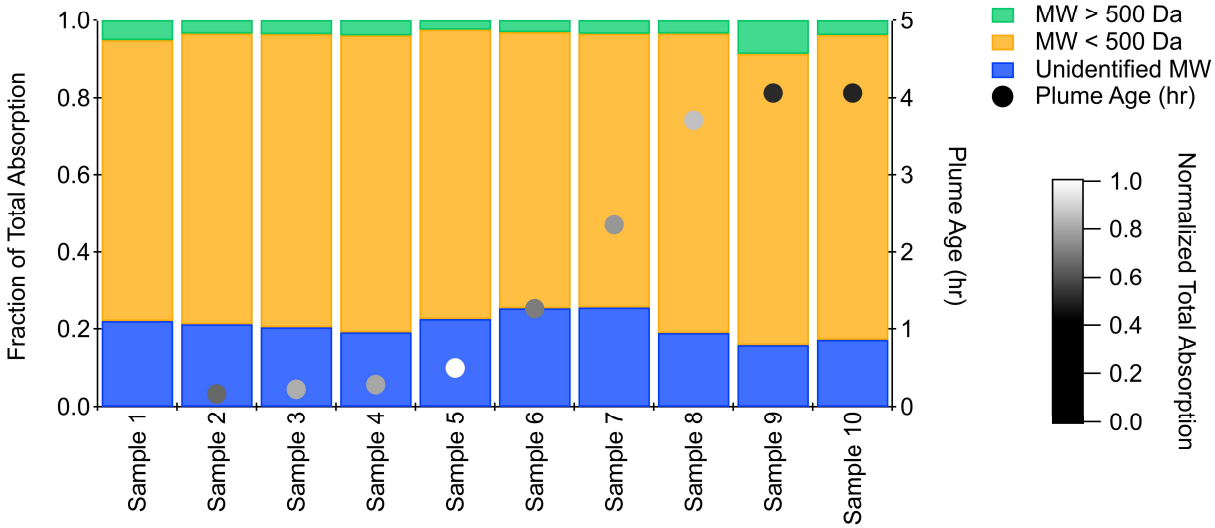

742

743 **Figure 3.**

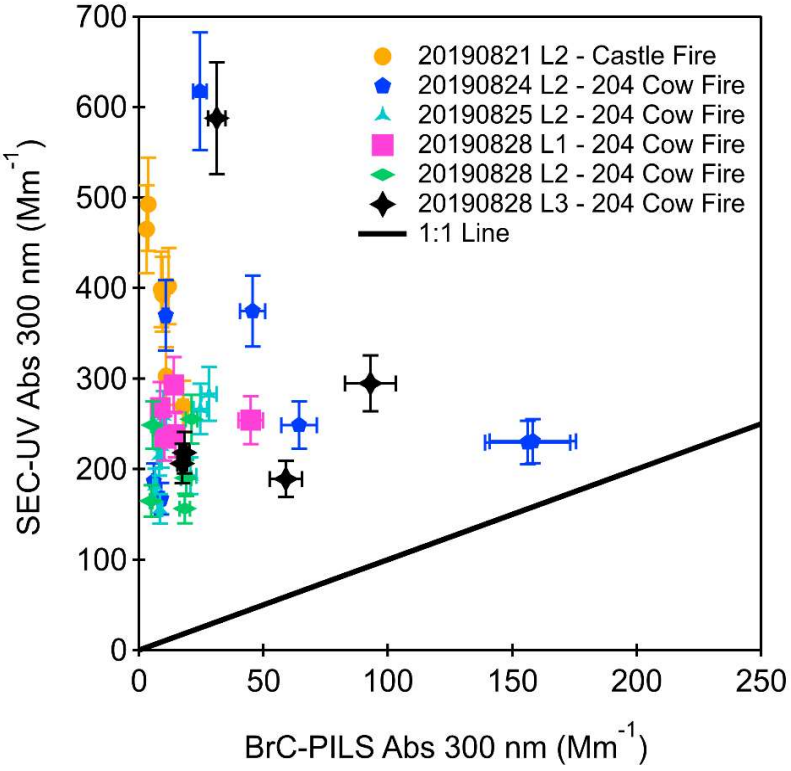

744

Figure 4.

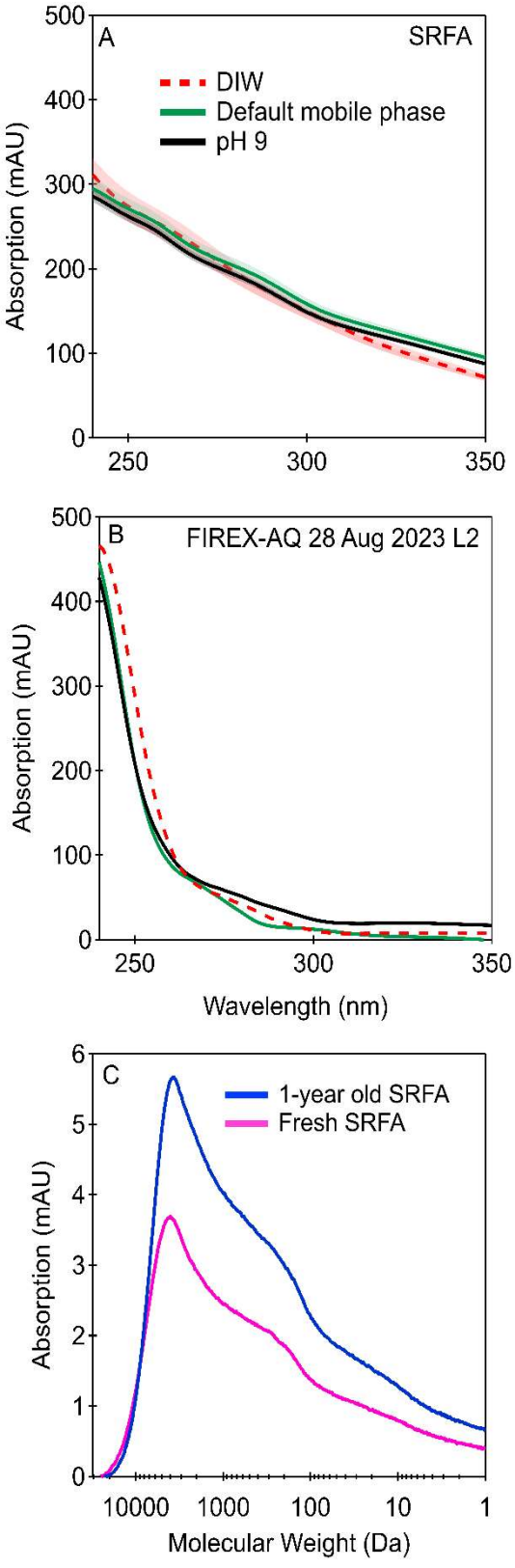
A
SRFA
DIW
Default mobile phase
pH 9
Absorption (mAU)
500
400
300
200
100
0
250
300
350
B
FIREX-AQ 28 Aug 2023 L2
Absorption (mAU)
Wavelength (nm)
C
1-year old SRFA
Fresh SRFA
Absorption (mAU)
6
5
4
3
2
1
0
10000
1000
100
10
1
Molecular Weight (Da)